Atmospheric Research 215 (2019) 116–127

Contents lists available at ScienceDirect

Atmospheric Research

journal homepage: www.elsevier.com/locate/atmosres

Human-perceived temperature changes over South China: Long-term trends and urbanization effects

Yijing Wang[a], Liutao Chen[a], Zhiying Song[a], Zeqing Huang[a], Erjia Ge[b], Lijie Lin[c], Ming Luo[a,d,*]

[a] School of Geography and Planning, and Guangdong Key Laboratory for Urbanization and Geo-simulation, Sun Yat-sen University, Guangzhou 510275, China.
[b] Dalla Lana School of Public Health, University of Toronto, Toronto, ON, Canada.
[c] School of Management, Guangdong University of Technology, Guangzhou 510520, China.
[d] Institute of Environment, Energy and Sustainability, The Chinese University of Hong Kong, Sha Tin, N.T., Hong Kong, China.

ARTICLE INFO

Keywords:
Human-perceived temperature
Heat stress
Wind chill
Long-term trend
Climate change
Urbanization effect

ABSTRACT

While the changes in air temperature under climate change and urbanization have been extensively examined in the literature, little is known about how human-perceived temperatures change. This study investigates the long-term changes in human-perceived temperatures (e.g., summer heat stress and winter wind chill conditions) over South China and quantifies the possible effects of urbanization. Daily observations at 86 stations during the period of 1961–2014 are collected and analyzed. Analysis results show that heat stress and wind chill temperature increase faster than air temperatures (i.e., daily mean, maximum, and minimum temperatures), and these increases are stronger in winter than in summer. The probabilities of hot extremes increase throughout the study period, whereas those of cold extremes decrease. Compared with those in non-urban areas, the warming trend in both seasons and the increase (decrease) in hot (cold) extremes are even more substantial in highly developed urban areas, such as the Pearl River Delta, indicating a remarkable effect of urbanization. It is estimated that urbanization contributes as much as half of the warming trend in summer and around one-third of the trend in winter. These results are helpful for mitigating climate change and reducing the impacts of extreme events.

1. Introduction

Under a warming climate, mean temperature and the intensity of extreme climate have been increasing all over the world, posing severe threats on ecosystems, water resource, food security, and human health (IPCC, 2012, 2013). The frequencies of extremes nonlinearly change with global mean air temperature (AT), and a small variation in the mean temperature may trigger a substantial change in extremes (Meehl et al., 2000; IPCC, 2013; Matthews et al., 2017). Therefore, extreme temperatures in many regions exhibit even more prominent warming trend than mean temperature. Specifically, many studies have demonstrated the increasing extremely hot events and decreasing cold events since the 1950s (IPCC, 2014; Luo and Lau, 2017; Nasim et al., 2018). Other studies also revealed that solar activity might modulate the changes in surface climate over a long time scale (Shindell et al., 2001; Romanic et al., 2018).

Studies have attributed the changes in hot and cold thermal conditions to adverse human health outcomes (Kunkel et al., 1999; McMichael et al., 2006). In summer, people may have an acute response to heat conditions; conversely, they may have a lag physiological response to environmental conditions in winter (Allen and Sheridan, 2014). Temperature has a close relationship with mortality, which considerably rises when temperature either increases or decreases (Baccini et al., 2008; Ye et al., 2012; Ma et al., 2014; Gasparrini et al., 2015). Both hot and cold extremes largely impact human health. For example, hot extreme is a major cause of heatstroke, exhaustion, cramps, syncope, and respiratory diseases, among others (Ma et al., 2015; Gronlund et al., 2016). Humans are prone to frostbite when exposed to severe cold conditions even for a short time (Hassi, 2005; Fallahi et al., 2017). These extremes can also increase the risk of mortality especially for the elderly, children, and persons with chronic medical conditions in many countries (Schwartz, 2005; Xu et al., 2012; Zanobetti et al., 2012).

Human-perceived temperature describes the “feels-like” equivalent temperature by considering the joint effects of temperature, humidity, and wind velocity (Epstein and Moran, 2006; Oleson et al., 2015). Recent studies show that human-perceived apparent temperature increases faster than AT, and the impacts of thermal discomfort on human

* Corresponding author at: Ming Luo, School of Geography and Planning, Sun Yat-sen University, Guangzhou 510275, China.
E-mail address: luom38@mail.sysu.edu.cn (M. Luo).

https://doi.org/10.1016/j.atmosres.2018.09.006
Received 28 March 2018; Received in revised form 31 August 2018; Accepted 5 September 2018
Available online 06 September 2018
0169-8095/

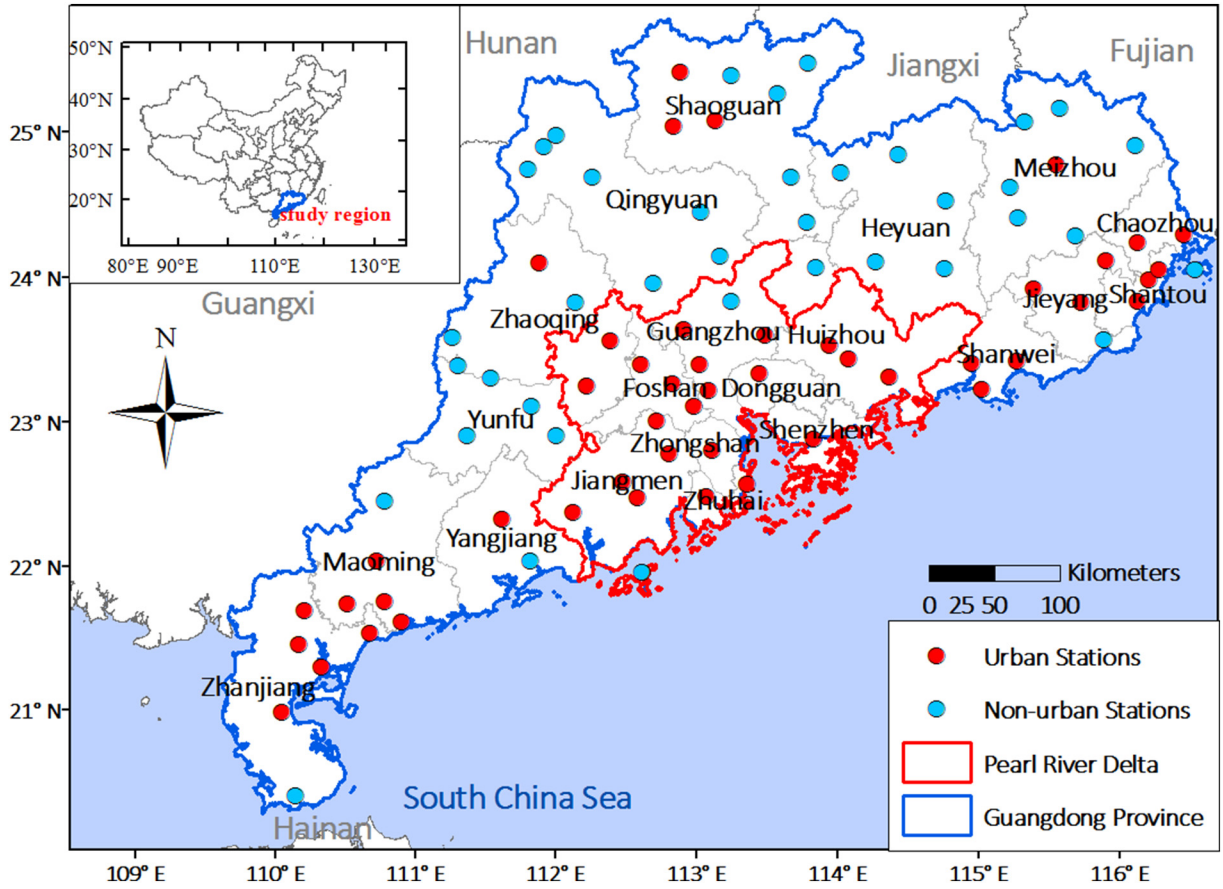

Fig. 1. Location of meteorological stations in Guangdong Province of South China. Urban and non-urban stations are depicted by red and blue circles respectively. The Pearl River Delta (PRD) is denoted by the red boundary. (For interpretation of the references to colour in this figure legend, the reader is referred to the web version of this article.)

Table 1
Definitions of temperature indicators used in this study.

Indicators		Definition	Unit
Mean	HI	Heat index	℃
	WCT	Wind chill temperature	℃
	T	Daily mean temperature	℃
	TX	Daily maximum temperature	℃
	TN	Daily minimum temperature	℃
Extreme	HI90p	Percentage of days when HI > 90th percentile (extremely heat stress day)	%
	TX90p	Percentage of days when TX > 90th percentile (extremely hot day)	%
	TN90p	Percentage of days when TN > 90th percentile (extremely hot night)	%
	WCT10p	Percentage of days when WCT < 10th percentile (extremely wind chill night)	%
	TX10p	Percentage of days when TX < 10th percentile (extremely cold day)	%
	TN10p	Percentage of days when TN < 10th percentile (extremely cold night)	%

health are increasingly becoming evident (Matthews et al., 2017; Lee and Min, 2018; Li et al., 2018). The joint environmental effects of ambient temperature, radiation, humidity, and air movement are contributing factors to human thermal comfort (Epstein and Moran, 2006). Extreme perceived temperatures, including heat stress and wind chill, can potentially reduce labor capacity and lead to extreme-related diseases and even deaths (Dunne et al., 2013). Therefore, the variations in human-perceived temperature should be investigated.

China has the largest population in the world and is vulnerable to climate change and climate extremes (Liu et al., 2015). Many studies in China have focused on the variation in extreme climate events (Zhai and Pan, 2003; Zhou and Ren, 2011; Zhou et al., 2016; Zhang et al., 2017b; Luo and Lau, 2018). The average temperature in China increased by 0.9 °C–1.5 °C from 1909 to 2011, which is higher than the global average trend (Liu et al., 2015). Climate warming in China is mainly manifested in winter, and winter is warming faster than the three other seasons (Ren et al., 2005; Ding et al., 2007). However, the changes in human-perceived temperature have not been unraveled yet.

The prominent warming trend over China can be accelerated by its rapid urbanization. Urbanization plays a key role in transforming natural environment to other land uses, thereby increasing the areas of impermeable ground and changing atmospheric process (Zhou et al., 2004; Wang and Yan, 2016). As a result, this phenomenon exerts essential influences on local climate change and extreme temperatures (Yang et al., 2011; Ren and Zhou, 2014; Sun et al., 2014; Sun et al., 2016). The largest and highly developed urban agglomerations with a dense population and significant economic status in China, such as the Yangtze River Delta (YRD), the Pearl River Delta (PRD), and the Beijing–Tianjin–Hebei (BTH) region, suffer severe impacts of climate extremes (Sun et al., 2014; Peng et al., 2017; Zhang et al., 2017a). Compared with those in YRD and BTH, urbanization effects (UEs) on local climate change in South China have not been investigated extensively (Xiong et al., 2012; Luo and Lau, 2017).

Hot extremes frequently occur in summer in South China, whereas cold extremes occasionally appear in winter. Hot and cold extremes pose negative impacts on public health in this area (Du and Xu, 2013). For example, the 2004 heat wave in Guangzhou caused 39 deaths, and the 2008 cold spell in South China resulted in even more respiratory

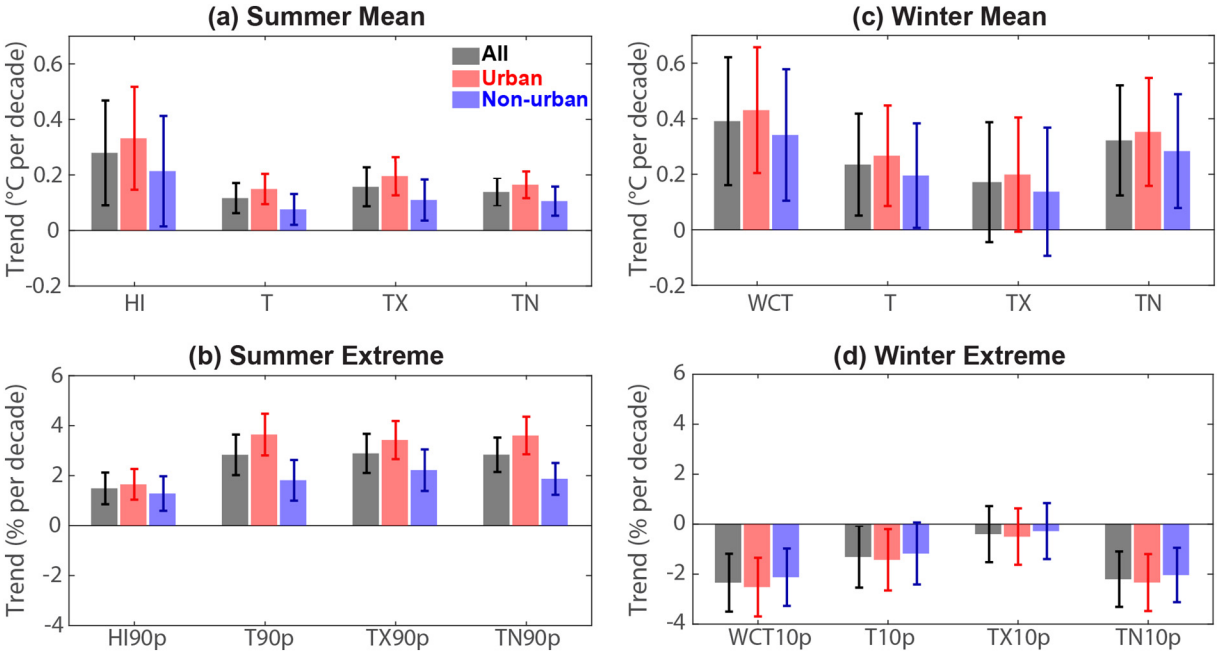

Fig. 2. Trends of mean (top) and extreme (bottom) temperatures in the summer (left) and winter (right) seasons of South China during the period of 1961–2014. Gray, pink, and blue colors indicate the trends for all, urban, and non-urban stations, respectively. Vertical error bar denotes the 95% confidence interval, as obtained by the modified Mann-Kendall trend test (Hamed and Rao, 1998). (For interpretation of the references to colour in this figure legend, the reader is referred to the web version of this article.)

fatalities (Du et al., 2013). Previous studies have mainly focused on actual AT and neglect the changes in human-perceived temperature, an indicator that is directly related to human health. The possible influences of local urbanization on perceived temperature changes over South China also remain unclear.

Therefore, this study aims to investigate the changes in perceived temperature over South China and quantify the possible effects of urbanization. This investigation is helpful for understanding the variation in weather events directly associated with human health. By revealing the relationship between urbanization and the occurrences of extreme climate events, we can potentially improve the accuracy of the forecast and prediction for these events. Accordingly, useful implications can be provided to local governments for formulating policies to mitigate climate change and extremes.

The remainder of the paper is structured as follows. Section 2 introduces the data and methods used in this study. Section 3 examines the changes in mean and extreme temperatures. Section 4 analyzes the influences of urbanization on these changes. Sections 5 and 6 present the discussion and conclusions, respectively.

2. Data and methodology

2.1. Study region

This study takes Guangdong Province as an example to investigate the changes in perceived temperature over South China. Guangdong Province is located in the southern coastal area of China (Fig. 1), and it has a long hot and wet summer (i.e., May–September) and relatively short chilly winter (i.e., December–February). Guangdong has had the highest GDP among all provinces of mainland China since 1989. The urbanization level of Guangdong Province was 68% in 2014, which is > 13% of the national mean. PRD (as denoted by a rectangular box in Fig. 1) is one of the largest and most highly developed urban agglomerations in eastern China, and its urbanization level reaches 84.12% (Statistics Bureau of Guangdong Province, 2014).

2.2. Data

Daily mean (T hereinafter), maximum and minimum temperatures (TX and TN), relative humidity (RH), and wind velocity (V) at 86 meteorological stations in Guangdong spanning from 1961 to 2014 are collected from the China Meteorological Data Service Center at http://data.cma.cn. The raw data are homogenized by a method as described by Xu et al. (2013). As shown in Fig. 1, the stations are nearly evenly distributed across the study region.

To estimate the possible effects of urbanization, we identify urban and non-urban stations based on the urban areas as extracted from the DeLorme World Base Map dataset. The dataset is obtained from the Baruch College Newman Library, The City University of New York at https://www.baruch.cuny.edu/confluence/display/geoportal/ESRI+International+Data (assessed in December 2017). Note that not all urban areas in this dataset have a very large population, and some urban areas may have relatively small population. As suggested by Mishra et al. (2015), we thus focus the urban areas with a population higher than 250,000, and stations located within 25-km of these urban areas are classified into urban type while the others are categorized as non-urban type. The urban areas are verified with the urban extents derived from the MODIS satellite data (Schneider et al., 2009; Mishra et al., 2015), and the comparison results show that the urban areas with > 250,000 population are located within the MODIS-based urban extents.

2.3. Perceived temperature indicators

We adopt the heat index (HI) (Rothfusz, 1990) and wind chill temperature (WCT) (Osczevski and Bluestein, 2005) to measure heat and cold perceived temperatures, respectively. To compare air and perceived temperatures, we also examine the changes in T, TX, and TN (Table 1). RH and V are used to calculate summer HI and winter WCT, respectively. Six extreme temperature indices are also used, three of them are related to hot extremes (TX90p, TN90p, and HI90p), and the three others are related to cold extremes (TX10p, TN10p, and WCT10p). The definitions of the indices are summarized in Table 1.

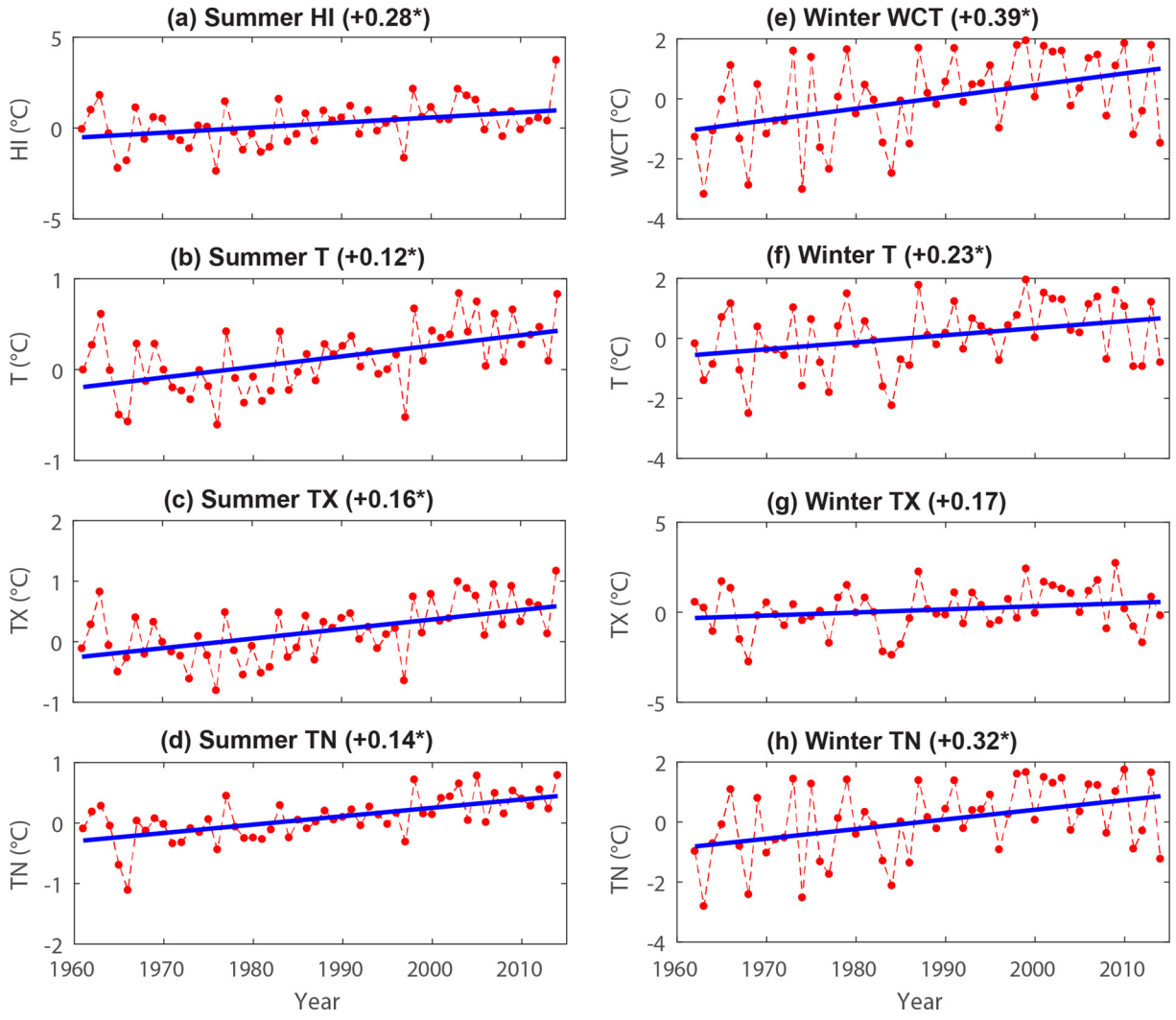

Fig. 3. Time series of summer (left) and winter (right) mean temperatures averaging for all stations. Straight lines denote the corresponding linear trends. Asterisk denotes significance at the 0.05 level.

Table 2
Trends of temperature indicators for all, urban, and non-urban stations during 1961–2014. Bold denotes significance at the 0.05 level.

Indicators	Summer				Winter			
	All	Urban	Non-urban	UE	All	Urban	Non-urban	UE
HI/WCT	**+0.28**	**+0.33**	**+0.22**	+0.11	**+0.39**	**+0.43**	**+0.33**	+0.10
T	**+0.12**	**+0.15**	**+0.07**	+0.08	**+0.23**	**+0.27**	+0.19	+0.08
TX	**+0.16**	**+0.20**	**+0.11**	+0.09	+0.17	+0.21	+0.13	+0.08
TN	**+0.14**	**+0.16**	**+0.10**	+0.06	**+0.32**	**+0.36**	**+0.28**	+0.12
HI90p/WCT10p	**+1.49**	**+1.65**	**+1.28**	+0.37	**−2.34**	**−2.52**	**−2.12**	−0.40
T90p/T10p	**+2.83**	**+3.64**	**+1.81**	+1.83	−1.31	−1.43	−1.17	−0.26
TX90p/TX10p	**+2.89**	**+3.42**	**+2.22**	+1.20	−0.40	−0.50	−0.28	−0.22
TN90p/TN10p	**+2.83**	**+3.60**	**+1.87**	+1.73	**−2.20**	**−2.34**	**−2.04**	−0.30
RH	**−0.72**	**−0.93**	**−0.46**	−0.47	**−0.78**	**−0.99**	−0.52	−0.47
V	**−0.04**	**−0.07**	−0.00	−0.07	**−0.08**	**−0.11**	**−0.04**	−0.07

Specifically, HI (°C) is computed using the algorithm by AT (°C) and RH (%) as follows (Rothfusz, 1990):

$$HI = -8.7847 + 1.6114 \times AT - 0.012308 \times AT^2 + RH \times (2.3385 - 0.14612 \times AT + 2.2117 \times 10^{-3} \times AT^2) + RH^2 \times (-0.016425 + 7.2546 \times 10^{-4} \times AT - 3.582 \times 10^{-6} \times AT^2)$$

WCT represents human-perceived temperature lower than AT because of the flow of wind (Osczevski and Bluestein, 2005). This index has been widely used to study the spatial and temporal changes in winter chill conditions (Howarth and Laird, 2017). WCT (°C) under windy conditions (i.e., $-50\,°C \le AT \le 10\,°C$ and $V \ge 5$ km/h) is calculated as

$$WCT = 13.12 + 0.6215 \times AT - 11.37 \times V^{0.16} + 0.3965 \times AT \times V^{0.16}.$$

Meanwhile, WCT with small wind speed (i.e., < 5 km/h) is calculated by (Mekis et al., 2015)

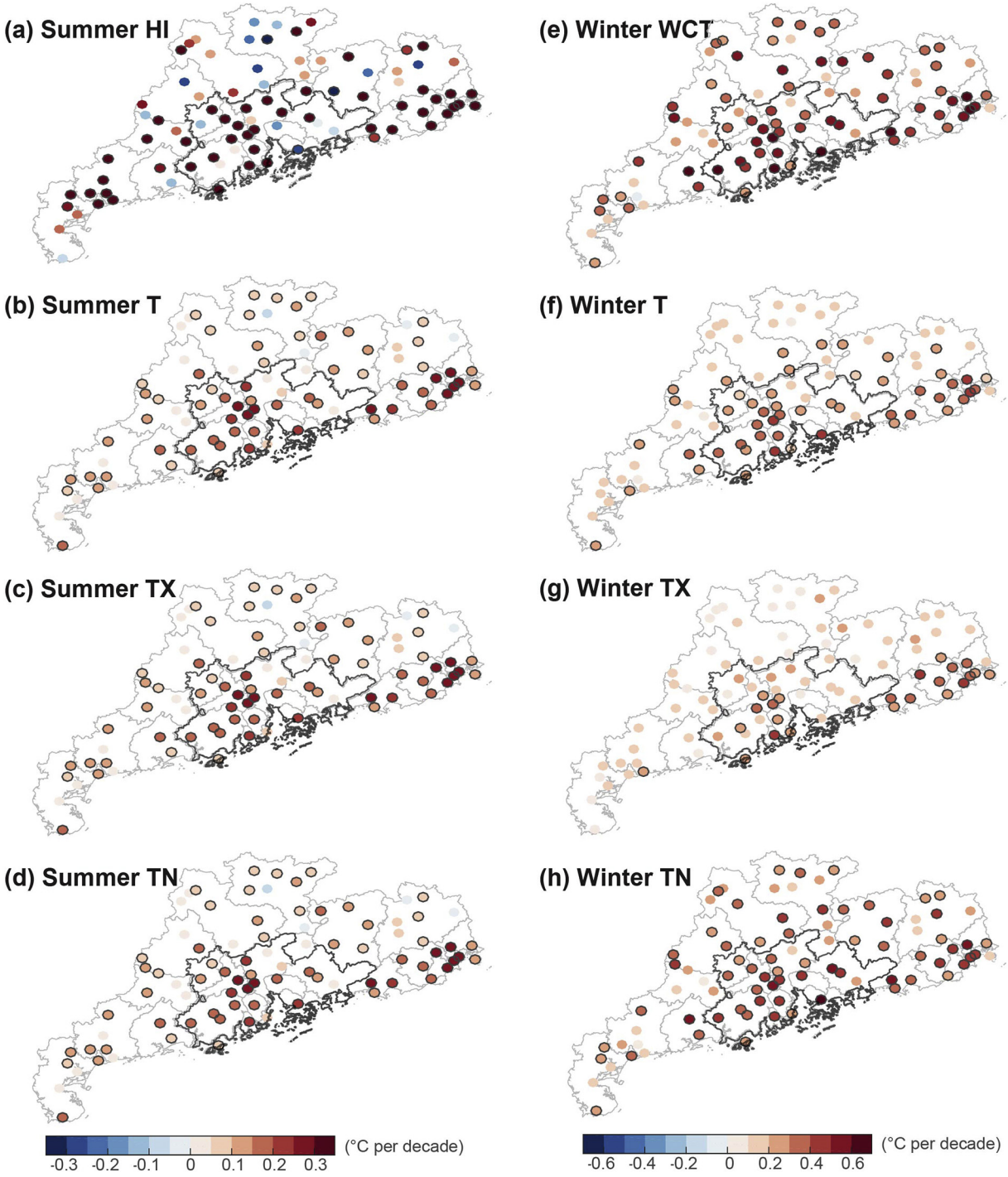

Fig. 4. Spatial distributions of trends of summer (left) and winter (right) mean temperatures. Black circle denotes significance at the 0.05 level. The dark-gray boundary denotes the PRD area. (For interpretation of the references to colour in this figure legend, the reader is referred to the web version of this article.)

$$WCT = AT + (-1.59 \times V + 0.1345 \times AT \times V)/5.$$

WCT is calculated for 54 winters (i.e., December–February) and 1961/62 winter refers to December 1961 to February 1962, and so forth.

2.4. Statistical analysis

The monthly anomalies of mean temperature indicators (i.e., T, TX, TN, HI, and WCT) are calculated by removing the multi-year climatological mean over the reference period of 1971–2000, and seasonal anomalies are obtained by averaging monthly anomalies in the corresponding season. The secular trends of the mean and extreme indicators are estimated by simple linear regression. The existence of significant trends is evaluated by the modified nonparametric Mann–Kendall (mMK) test (Hamed and Rao, 1998). The 95% confidence intervals are calculated as the middle 95% of the slopes of lines determined by pairs of points. Compared with the original MK version, the mMK method considers the autocorrelation in the time series, thereby providing an unbiased evaluation of the trend. The mMK method has been widely used in previous hydrological and climatological studies (Radinović and Ćurić, 2012). Details of the mMK method can be found in Hamed and Rao (1998).

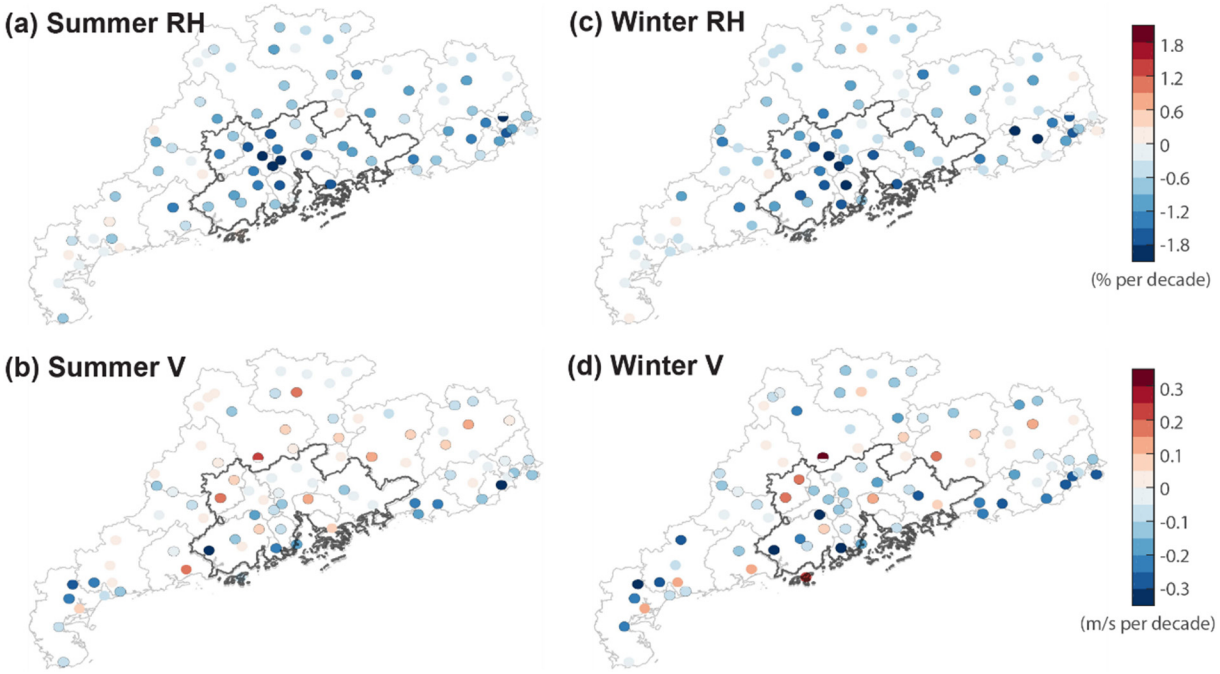

Fig. 5. Same as Fig. 4 but for (top) RH and (bottom) V.

3. Long-term changes

3.1. Changes in mean temperatures

The long-term trends of mean temperatures during the period of 1961–2014 are given in Fig. 2. Fig. 3 illustrates the evolution of summer mean temperatures in Guangdong. Despite some fluctuations, HI, T, and its TX and TN show overall upward trends throughout this period with values of 0.28 °C, 0.12 °C, 0.16 °C, and 0.14 °C decade^{-1}, respectively (Fig. 2 and Fig. 3a–d). The increasing trend of HI is larger than that of T, TX, and TN, suggesting that summer perceived temperature warms faster than AT. In addition, the trend of TN is slightly weaker than that of TX, indicating that daytime temperature increases faster than nighttime temperature. This result is consistent with that in Ye et al. (2018). One possible reason is that summer precipitation over South China has been increasing during the past decades (Zhai et al., 2005; Ye et al., 2013; Ye, 2014), and the increasing soil moisture associated with the increase of rainfall can slow down the TN warming (Zhou et al., 2007; Cheng et al., 2015). RH decreases by 0.72% decade^{-1}, and V weakens considerably during the period of 1961–2014 by 0.04 m/s decade^{-1} (Table 2).

The trends of these indicators in summer at 86 stations can be adapted into a map-based regional assessment presented in Fig. 4. These maps demonstrate the spatial variations in these variables. As shown in Fig. 4a, HI at nearly all stations (80.2%) has increasing trends. These trends are considerably prominent in urbanized areas, suggesting that urbanization exerts intensifying effects on summer heat stress over South China. As shown in Fig. 4b, T at nearly all stations (95.3%) rises during the past 54 years. In particular, T in the PRD, Chaoshan (including Chaozhou, Shantou, and Jieyang), and southwest coastal areas warms faster than that in other areas. These areas are also densely populated and highly urbanized, implying that urbanization remarkably contributes to the warming summer climate in Guangdong Province. Similar to T, TX and TN are increasing in most parts of Guangdong, particularly in PRD and eastern coastal area (Fig. 4c–d). In the case of humidity (Fig. 5a), RH decreases in most portions, indicating that Guangdong is relatively dry. The most severely “drying” regions are again the highly urbanized areas, such as PRD and Chaoshan. As shown in Fig. 5b, V exhibits distinctive regional differences with an increasing trend at several stations in inland areas and a declining trend at coastal stations.

Temperatures in 53 winters during the period of 1961–2014 by averaging 86 surface stations are demonstrated in the right column of Fig. 3. T, TX, and TN show obvious upward trends with values of 0.23 °C, 0.17 °C, and 0.32 °C decade^{-1}, respectively (Fig. 3f–h). These trends are much stronger than those in summer (i.e., 0.12 °C, 0.16 °C, and 0.14 °C decade^{-1}). This finding agrees with the results of previous studies (Lin et al., 1995; Wang et al., 2004; Ren et al., 2005). Lin et al. (1995) concluded that the climate warming in China is mainly manifested in winter. V plumbs radically (-0.08 m/s decade^{-1}), indicating that wind strength is weakening (Fig. 5d). Compared with that in the summertime (-0.04 m/s decade^{-1}), the trend in winter is stronger as well. The weakening of the winter monsoon circulation is more evident than that of the summer monsoon circulation, and the weakening of the winter and summer monsoon circulations reveals the physical connotation of the weakening of wind speed over China (Wang et al., 2004; Ren et al., 2005; Xu et al., 2006; Feng et al., 2009). Furthermore, WCT (Fig. 3e) has a stronger increasing trend than temperatures and rises considerably by 0.39 °C decade^{-1}, and such phenomenon may decrease V.

The spatial patterns of WCT, T, TX, and TN trends are shown in Fig. 4e–h. All temperatures show upward trends in all parts of Guangdong. As shown in Fig. 4e, the increasing trend of WCT is especially strong in the densely populated and highly urbanized areas, such as PRD and Chaoshan. The maps of T, TX, and TN show their upward tendencies over Guangdong Province (Fig. 4f–h). T and TX climb in the central part of the province and coastal area. TN rises in the majority of the province, and its increase is stronger than those of T and TX, indicating that nighttime temperature warms faster than the daytime one. RH (Fig. 5c) plunges in nearly the entire area (94.2%), and the trends in the PRD and Chaoshan areas are noticeably prominent than those in other areas. The spatial distribution of V is relatively complex and heterogeneous (Fig. 5d). In particular, V shows a decreasing trend in coastal areas and an increasing trend in parts of inland areas. This combined effect of rising temperature and declining wind speed over South China from 1956 to 2005 has also been reported by Feng et al. (2009).

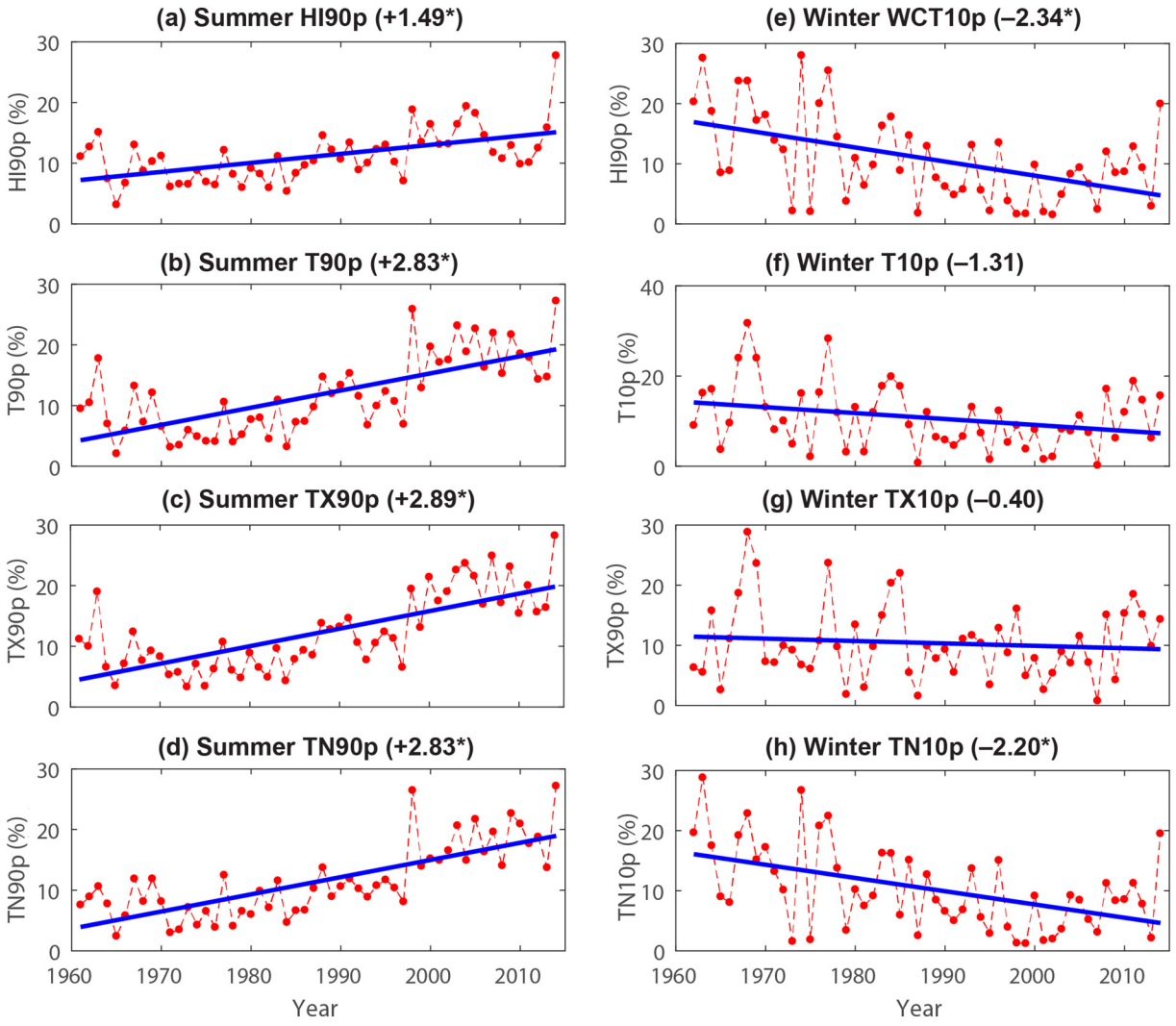

Fig. 6. Same as Fig. 3 but for extreme temperature indices.

3.2. Changes in extreme temperatures

Ts in summer and winter show profound warming trends. In this subsection, we analyze the changes in extreme temperatures. The results are shown in Fig. 6 and Fig. 7. As depicted in the left column of Fig. 6, all indicators for summer hot extremes (i.e., HI90p, T90p, TX90p, and TN90p) rise dramatically during the past decades. The trends of HI90p, T90p, TX90p, and TN90p are 1.49%, 2.83%, 2.89%, and 2.83% decade^{-1}, respectively (Fig. 6a–d). Although HI90p has an increasing trend, this trend is smaller than those of T90p, TX90p, and TN90p. These results suggest that the number of extremely hot days and nights is increasing in South China, and the weather is becoming warmer than before.

Fig. 7 depicts the distribution of temperature extreme trends. HI90p increases at 70 stations (81.40%), and most of them are located in the PRD and Chaoshan areas (Fig. 7a). T90p (96.51%), TX90p (98.84%), and TN90p (95.35%) at nearly all stations increase, and they rise substantially in urbanized areas (Fig. 7b–d). This result suggests that urbanization has a profound impact on intensifying hot extremes.

In the winter season (right column of Fig. 6), WCT10p, T10p, TX10p, and TN10p show overall decreasing trends. The probability of extreme chill days (WCT10p) shows a steep drop with a value of 2.34% decade^{-1} (Fig. 6e). This drop is remarkably stronger than those of the three other indices. The downward trend of T10p is 1.31% decade^{-1}, whereas TX10p and TN10p decrease by 0.40% and 2.20% decade^{-1}, respectively (Fig. 6f–h). Therefore, the frequencies of extremely cold days and nights decline, and cold night declines even more dramatically than that of cold day. These findings are consistent with those of IPCC (2014). The decline in cold extremes is resembled with the weakening in V (Fig. 4d), which is in line with a previous study (Wang et al., 2004).

The maps in Fig. 7e–h illustrate that nearly all parts of the area are experiencing decreasing cold extremes. These decreases are particularly substantial in the PRD and Chaoshan areas, implying a considerable effect of urbanization. All cold extremes show considerable differences between developed and developing areas. The effects of urbanization on these changes are investigated in the following section.

4. Urbanization effects

4.1. Urbanization effects on mean temperatures

The results above imply that the changes in mean and extreme temperatures in South China may be affected by urbanization. In this section, we proceed to quantify the UE by classifying urban and non-urban areas.

The yearly evolutions of all temperature indicators calculated separately for urban and non-urban stations are shown in Fig. 8. Urban and non-urban series exhibit similar yearly variation in this period; conversely, their trends have discernable differences. In spite of some fluctuations, HI, T, TX, and TN increase considerably, and the

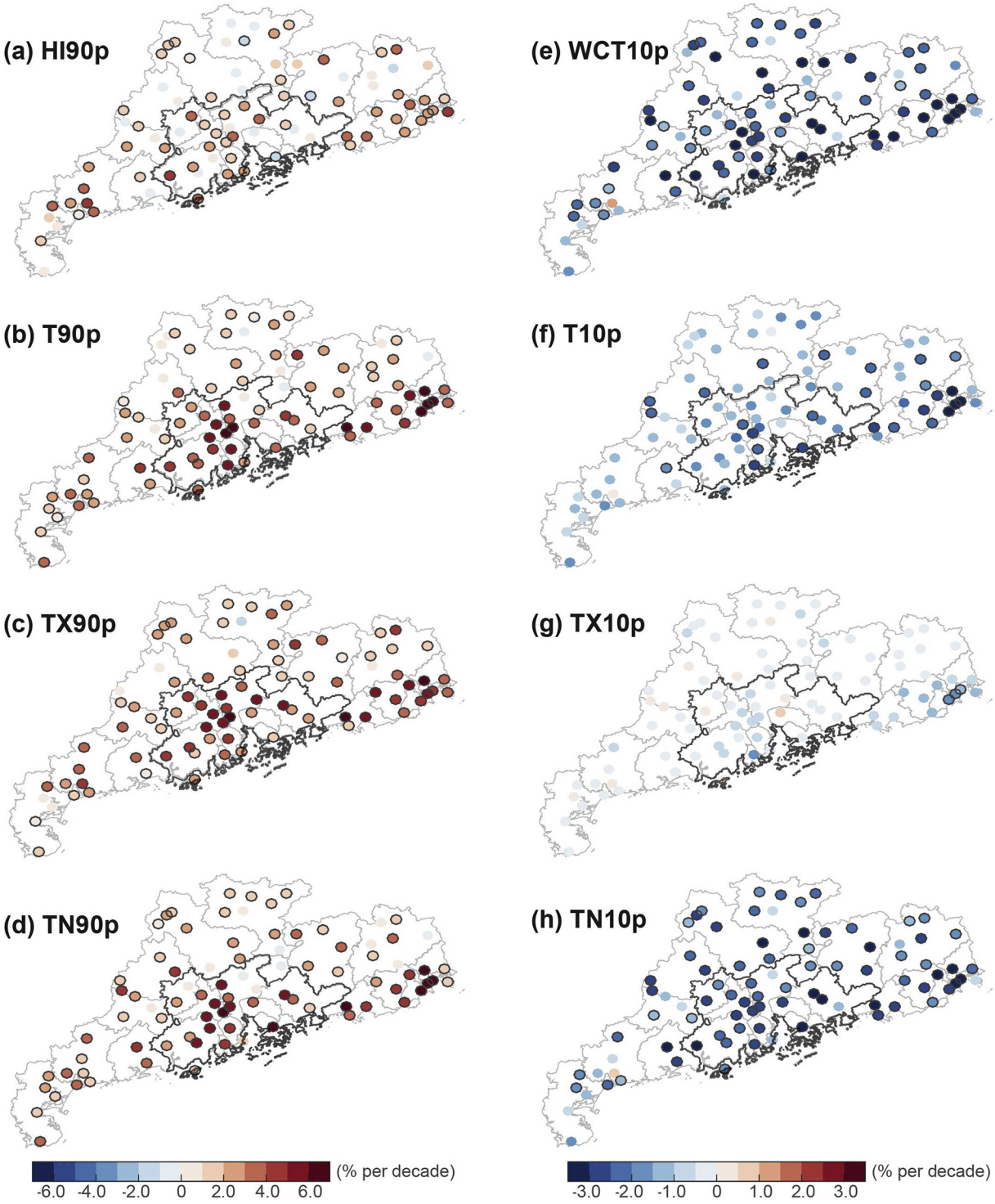

Fig. 7. Same as Fig. 4 but for extreme temperature indices.

increasing trends in urban areas are stronger than those in non-urban areas (Fig. 8a–d). HI in urban area bears an intensifying trend of 0.33% decade^{-1}, whereas non-urban HI increases by 0.22% decade^{-1}. These results indicate that urbanization induces an additional warming of 0.11% decade^{-1}, which accounts for 33.33% of the total warming trend. T, TX, and TN in urban areas increase faster than those in non-urban areas, and urbanization contributes to around 50.00% (0.08%, 0.09%, and 0.06% decade^{-1}, respectively). These contributions are larger than those of HI possibly due to that RH decreases faster in urban areas than in non-urban areas (see also Fig. 5a, c). The decreasing trend of urban RH is twice as much as that of non-urban RH. V decreases remarkably, and the decreasing trends in urban areas are stronger than those in non-urban areas (Fig. 5b, d). This phenomenon is associated with the intensification of surface friction by land use changes (Xu et al., 2006; Vautard et al., 2010).

In winter (Fig. 8e–h), all temperature trends are similar to those in summer; specifically, considerable warming is observed in all four temperature indicators. Compared with T, TX, and TN, WCT presents a steeper increase (0.39% decade^{-1}, Table 2). For urban and non-urban areas, the nighttime temperature climbs more noticeably than daytime

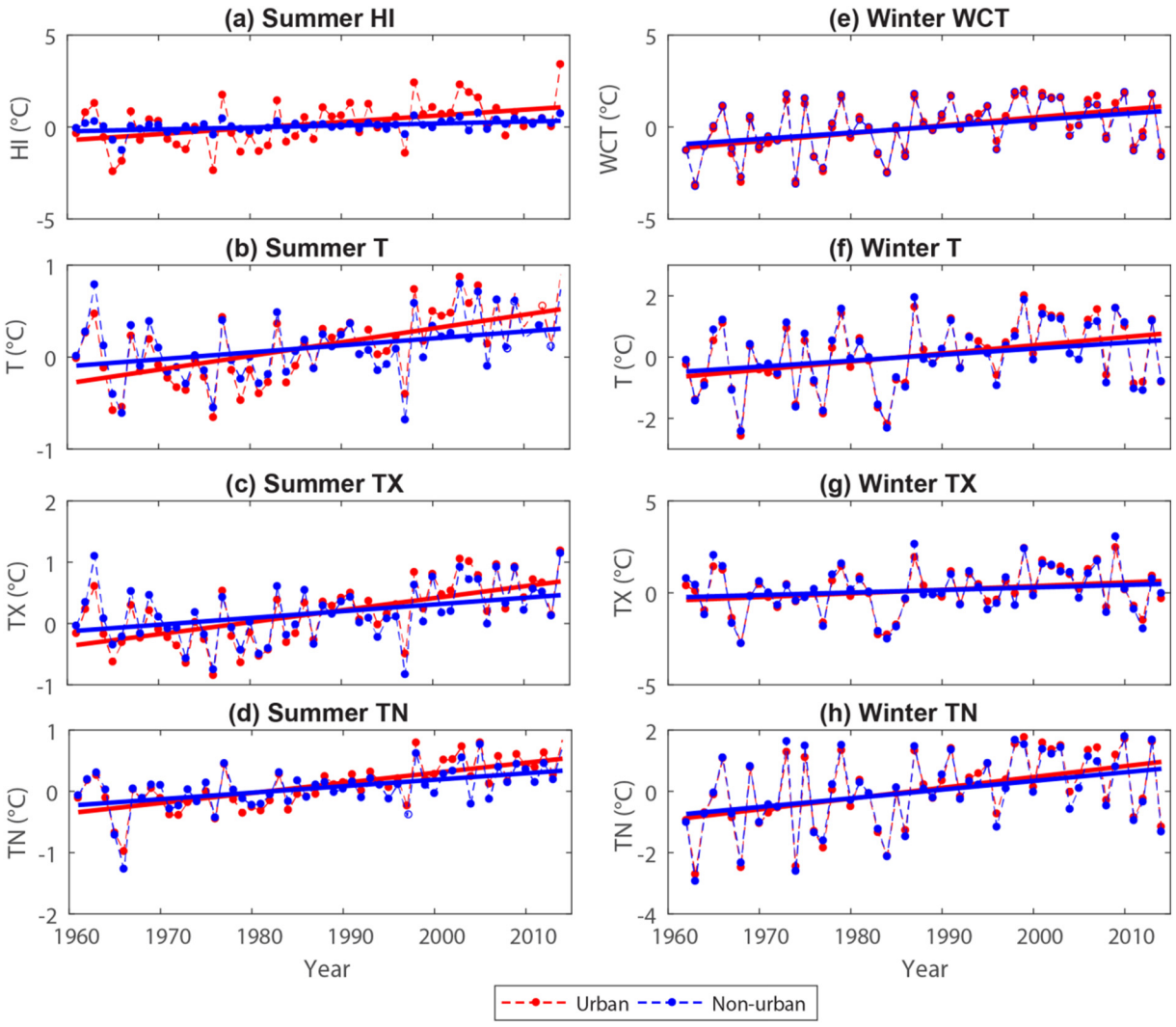

Fig. 8. Time series of summer (left) and winter (right) mean temperatures averaging for (red) urban and (blue) non-urban stations. (For interpretation of the references to colour in this figure legend, the reader is referred to the web version of this article.)

temperature (comparison of TX and TN, Fig. 2 and Table 2). These increases in non-urban areas are nearly one-third slower than those in urban areas.

4.2. Urbanization effects on extreme temperatures

Fig. 9 shows the differences in extreme temperatures between urban and non-urban areas. Hot extremes in summer in urban and non-urban areas increase considerably throughout the period of 1961–2014 (Fig. 9a–d), and the trends in non-urban areas are much weaker than those in urban areas. Moreover, the gap of HI90p between urban and non-urban areas is narrower than that of T90p, TX90p, and TN90p, suggesting that the UE on HI90p is smaller than the UE on others. The possible reason is explained as follows. Higher temperature extremes are usually accompanied by smaller RH because saturated water vapor (E_S) may increase faster than water vapor (E) although E_S and E increase with warm temperature. As a result, part of the increase in HI90p may be offset by the reduction in RH.

In winter season (Fig. 9e–h), the frequencies of cold extremes in urban and non-urban areas decline. TN10p and WCT10p decrease more considerably than T10p and TX10p, indicating that the number of extremely cold nights decreases. WCT10p decreases radically, and the large decrease in WCT10p is related to the weakening V. This weakening is even stronger in urban areas. The disparities in cold extremes between urban and non-urban areas are narrower than those in summer, agreeing with our results on Ts. The probability of WCT10p declines by 2.52% decade^{-1} in urban areas and 2.12% decade^{-1} in non-urban areas. Urbanization contributes approximately 16% to the decrease in WCT10p. The rapid alteration of urbanization on the frequencies of extremely cold days and nights has also been found in other regions, such as India (Giri et al., 2015).

5. Discussion

The long-term changes in mean and extreme temperatures under global warming and local urbanization have been extensively documented in literature. However, only a few studies have examined the changes in human-perceived temperatures. These indicators chracterize the combined effects of temperature, humidity and wind, and have close associations with public health. In this study, we go beyond and examine the changes in human-perceived temperatures over South China, one of the most urbanized and densely populated regions in the world. Our study can provide a better understanding of the physiological impacts of global warming and local urbanization on human beings and is important for adapting and mitigating climate change at the regional scale.

In the past years, many studies have been devoted to examining regional climate change and the impacts of urbanization. However,

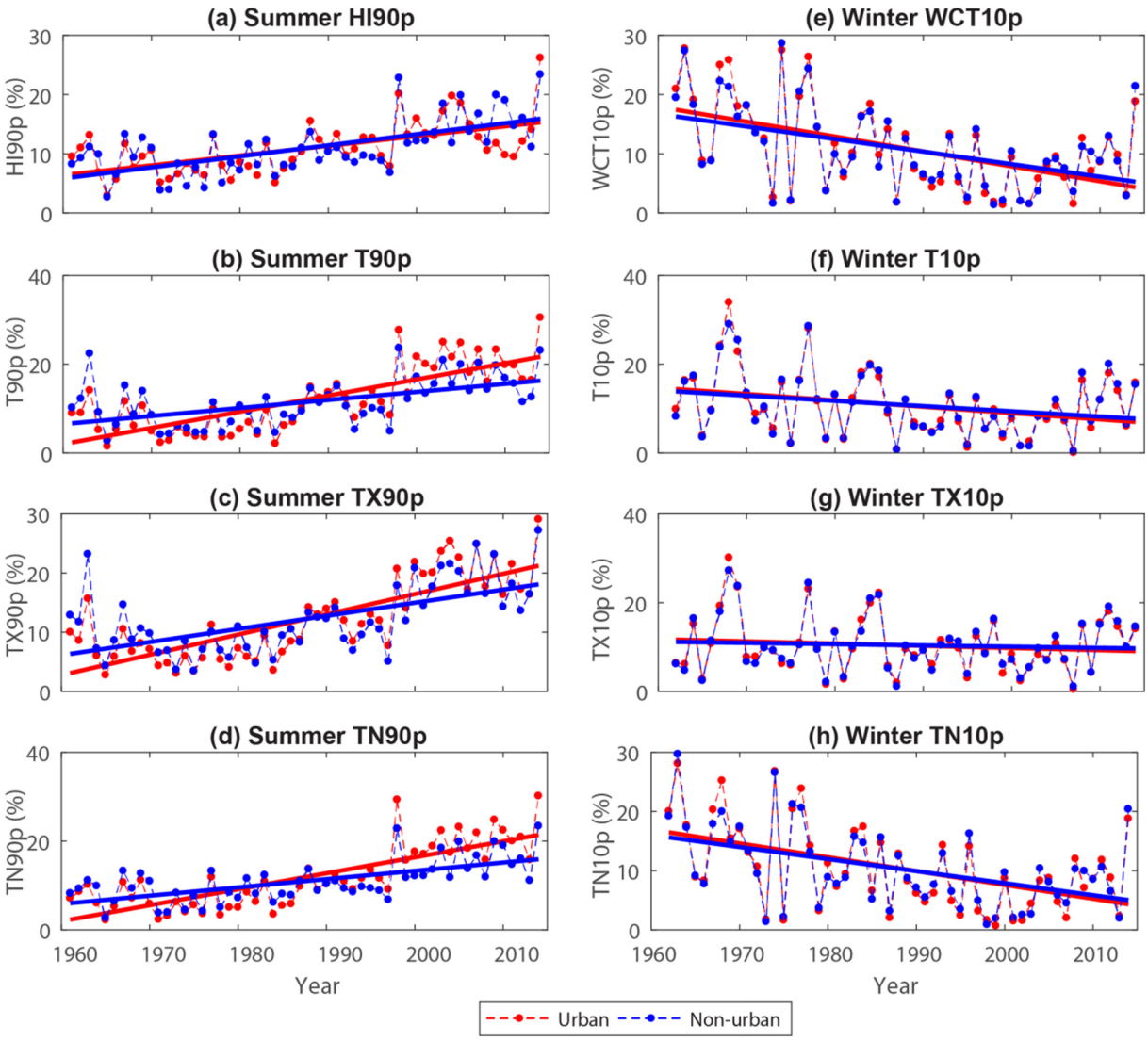

Fig. 9. Same as Fig. 8 but for extreme temperature indices.

these studies focus on the BTH and YRD regions (Ren et al., 2008; Gu et al., 2011; Si et al., 2014; Wang et al., 2015; Yang et al., 2017). Compared with these areas, the changing climate pattern in South China, as well as the possible impacts of urbanization on human-perceived temperatures, are less understood. Our analyses show that human-perceived temperatures have increased much faster than ATs during the past five decades and that urbanization can lead to nearly half of the increase in summer heat stress and one-third in winter wind chill. These results imply that human will perceive warmer thermal conditions under global warming and local urbanization than expected.

In our investigation, heat stress and winter chill are defined by HI and WCT, respectively. The two indicators have been widely used in climate change studies (Keimig and Bradley, 2002; Lobell et al., 2008; Oleson et al., 2015). Comparing our results with those based on other definitions, such as wet-bulb globe temperature and discomfort index, will be interesting (Epstein and Moran, 2006; Buzan et al., 2015). Extending the scope of our study by examining other parts of China is also interesting. Such examinations will provide a comprehensive understanding of the perceived temperature variations and possible effects of urbanization. These investigations shall be conducted in our future studies.

In the present study, the changes in perceived temperature and possible UE are investigated on the basis of observations. These changes can also be examined in model simulations. Further examinations of the output from simulations will reveal the associated processes underlying these changes. The projected changes in perceived temperature will be explored as well in the future.

6. Conclusion

This study provides a quantitative assessment of the changes in human-perceived temperatures (e.g., summer heat stress and winter wind chill) over South China and the possible influence of local urbanization on these changes with Guangdong Province as an example. The results uncovered here are helpful for guiding regional governments in mitigating climate change and extremes. The primary findings of this study are summarized as follows:

(1) During the period of 1961–2014, all T indicators in winter and summer seasons exhibit discernable warming trends across the study region, and winter temperatures show more profound trends than summer temperatures. Compared with other indicators (e.g., T, TX, and TN), summer HI and winter WCT show even stronger upward trends, suggesting that human-perceived temperatures increase faster than ATs.
(2) The frequencies of summer hot extremes increase dramatically,

whereas those of winter cold extremes decrease. Wind chill extremes (i.e., WCT10p) display steeper decreasing trend than AT extremes (i.e., T10p, TX10p, and TN10p) due to the weakening tendency in V.

(3) The warming in both seasons and the increasing (decreasing) trend in hot (cold) extremes are especially prominent in urbanized and populated areas, such as PRD and other coastal regions. Urbanization is estimated to contribute to half as much as of the warming trend in summer and around one-third in winter.

Acknowledgments

This study is funded by the National Natural Science Foundation of China (no. 41871029, 41401052, 51809294). The appointment of M. L. at Sun Yat-sen University is partially supported by the 100 Top Talents Program (Phase II).

References

Allen, M.J., Sheridan, S.C., 2014. High-mortality days during the winter season: comparing meteorological conditions across 5 US cities. Int. J. Biometeorol. 58 (2), 217–225.
Baccini, M., Biggeri, A., Accetta, G., et al., 2008. Heat effects on mortality in 15 European cities. Epidemiology 19 (5), 711–719.
Buzan, J., Oleson, K., Huber, M., 2015. Implementation and comparison of a suite of heat stress metrics within the Community Land Model version 4.5. Geosci. Model Dev. 8 (2), 151–170.
Cheng, S., Guan, X., Huang, J., et al., 2015. Long-term trend and variability of soil moisture over East Asia. J. Geophys. Res. Amos. 120 (17), 8658–8670.
Ding, Y., Ren, G., Shi, G., et al., 2007. China's national assessment report on climate change (I): climate change in China and the future trend (in Chinese). Adv. Clim. Chang. Res. 3, 1–5.
Du, Y., Xu, Y., 2013. Assess Report on Regional Climate Change in South China 2012: Summary for Policymakers. China Meteorological Press, Beijing, China.
Du, Y., Wang, X., Yang, X., et al., 2013. Impacts of climate change on human health and adaptation strategies in South China. Adv. Clim. Chang. Res. 4 (4), 208–214.
Dunne, J.P., Stouffer, R.J., John, J.G., 2013. Reductions in labour capacity from heat stress under climate warming. Nat. Clim. Chang. 3 (6), 563–566.
Epstein, Y., Moran, D.S., 2006. Thermal comfort and the heat stress indices. Ind. Health 44 (3), 388–398.
Fallahi, A., Reza Salimpour, M., Shirani, E., 2017. A 3D thermal model to analyze the temperature changes of digits during cold stress and predict the danger of frostbite in human fingers. J. Therm. Biol. 65, 153–160.
Feng, S., Gong, D., Zhang, Z., et al., 2009. Wind-chill temperature changes in winter over China during the last 50 years. Acta Geograph. Sin. 64, 1071–1082.
Gasparrini, A., Guo, Y., Hashizume, M., et al., 2015. Mortality risk attributable to high and low ambient temperature: a multicountry observational study. Lancet 386 (9991), 369–375.
Giri, R., Pradhan, D., Sen, A., 2015. Study of extreme weather events (hot & cold day or wave) over Bihar Region. Int. J. Appl. Eng. Technol. 5 (2), 67–84.
Gronlund, C.J., Zanobetti, A., Wellenius, G.A., et al., 2016. Vulnerability to renal, heat and respiratory hospitalizations during extreme heat among U.S. elderly. Clim. Chang. 136 (3), 631–645.
Gu, C., Hu, L., Zhang, X., et al., 2011. Climate change and urbanization in the Yangtze River Delta. Habit. Int. 35 (4), 544–552.
Hamed, K.H., Rao, A.R., 1998. A modified Mann-Kendall trend test for autocorrelated data. J. Hydrol. 204 (1–4), 182–196.
Hassi, J., 2005. Cold extremes and impacts on health. In: Kirch, W., Bertollini, R., Menne, B. (Eds.), Extreme Weather Events and Public Health Responses. Springer, Berlin, Heidelberg, pp. 59–67.
Howarth, M.E., Laird, N.F., 2017. Intraseasonal variations of winter wind chill temperatures across Canada and the United States. J. Appl. Meteorol. Climatol. 56 (11), 2951–2962.
IPCC, 2012. Managing the Risks of Extreme Events and Disasters to Advance Climate Change Adaptation: Special Report of the Intergovernmental Panel on Climate Change. Cambridge University Press, Cambridge, UK and New York, USA, pp. 582.
IPCC, 2013. Climate Change 2013: The Physical Science Basis. Contribution of Working Group I to the Fifth Assessment Report of the Intergovernmental Panel on Climate Change. Cambridge University Press, Cambridge, United Kingdom and New York, NY, USA, pp. 1535.
IPCC, 2014. Climate Change 2014–Impacts, Adaptation and Vulnerability: Regional Aspects. Cambridge University Press.
Keimig, F.T., Bradley, R.S., 2002. Recent changes in wind chill temperatures at high latitudes in North America. Geophys. Res. Lett. 29 (8) 4-1-4-4.
Kunkel, K.E., Pielke Jr., R.A., Changnon, S.A., 1999. Temporal fluctuations in weather and climate extremes that cause economic and human health impacts: a review. Bull. Am. Meteorol. Soc. 80 (6), 1077–1098.
Lee, S.-M., Min, S.-K., 2018. Heat stress changes over East Asia under 1.5° and 2.0°C global warming targets. J. Clim. 31 (7), 2819–2831.
Li, J., Chen, Y.D., Gan, T.Y., et al., 2018. Elevated increases in human-perceived temperature under climate warming. Nat. Clim. Chang. 8, 43–47.
Lin, X., Yu, S., Tang, G., 1995. Series of average air temperature over China for the last 100-year period. Sci. Atmos. Sin. 5, 423.
Liu, Y., Chao, Q., Ding, Z., 2015. Third National Climate Change Assessment Report of China. Science Press, Beijing, China.
Lobell, D.B., Bonfils, C.J., Kueppers, L.M., et al., 2008. Irrigation cooling effect on temperature and heat index extremes. Geophys. Res. Lett. 35 (9), L09705.
Luo, M., Lau, N.-C., 2017. Heat waves in southern China: synoptic behavior, long-term change, and urbanization effects. J. Clim. 30 (2), 703–720.
Luo, M., Lau, N.-C., 2018. Amplifying effect of ENSO on heat waves in China. Clim. Dyn. https://doi.org/10.1007/s00382-00018-04322-00380. in press.
Ma, W., Chen, R., Kan, H., 2014. Temperature-related mortality in 17 large Chinese cities: how heat and cold affect mortality in China. Environ. Res. 134, 127–133.
Ma, W.J., Zeng, W.L., Zhou, M.G., et al., 2015. The short-term effect of heat waves on mortality and its modifiers in China: an analysis from 66 communities. Environ. Int. 75, 103–109.
Matthews, T.K., Wilby, R.L., Murphy, C., 2017. Communicating the deadly consequences of global warming for human heat stress. Proc. Natl. Acad. Sci. U. S. A. 114 (15), 3861–3866.
McMichael, A.J., Woodruff, R.E., Hales, S., 2006. Climate change and human health: present and future risks. Lancet 367 (9513), 859–869.
Meehl, G.A., Karl, T., Easterling, D.R., et al., 2000. An introduction to trends in extreme weather and climate events: observations, socioeconomic impacts, terrestrial ecological impacts, and model projections. Bull. Am. Meteorol. Soc. 81 (3), 413–416.
Mekis, É., Vincent, L.A., Shephard, M.W., et al., 2015. Observed trends in severe weather conditions based on humidex, wind chill, and heavy rainfall events in Canada for 1953–2012. Atmos.-Ocean 53 (4), 383–397.
Mishra, V., Ganguly, A.R., Nijssen, B., et al., 2015. Changes in observed climate extremes in global urban areas. Environ. Res. Lett. 10 (2), 024005.
Nasim, W., Amin, A., Fahad, S., et al., 2018. Future risk assessment by estimating historical heat wave trends with projected heat accumulation using SimCLIM climate model in Pakistan. Atmos. Res. 205, 118–133.
Oleson, K., Monaghan, A., Wilhelmi, O., et al., 2015. Interactions between urbanization, heat stress, and climate change. Clim. Chang. 129 (3–4), 525–541.
Osczevski, R., Bluestein, M., 2005. The new wind chill equivalent temperature chart. Bull. Am. Meteorol. Soc. 86 (10), 1453–1458.
Peng, X., She, Q., Long, L., et al., 2017. Long-term trend in ground-based air temperature and its responses to atmospheric circulation and anthropogenic activity in the Yangtze River Delta, China. Atmos. Res. 195, 20–30.
Radinović, D., Ćurić, M., 2012. Criteria for heat and cold wave duration indexes. Theor. Appl. Climatol. 107 (3), 505–510.
Ren, G., Zhou, Y., 2014. Urbanization effect on trends of extreme temperature indices of national stations over mainland China, 1961–2008. J. Clim. 27 (6), 2340–2360.
Ren, G., Guo, J., Xu, M., et al., 2005. Climate changes of China's mainland over the past half century. Acta Meteorol. Sin. 63 (6), 942–956.
Ren, G., Zhou, Y., Chu, Z., et al., 2008. Urbanization effects on observed surface air temperature trends in North China. J. Clim. 21 (6), 1333–1348.
Romanic, D., Hangan, H., Ćurić, M., 2018. Wind climatology of Toronto based on the NCEP/NCAR reanalysis 1 data and its potential relation to solar activity. Theor. Appl. Climatol. 131 (1), 827–843.
Rothfusz, L.P., 1990. The Heat Index Equation (Or, More Than You Ever Wanted to Know About Heat Index). National Oceanic and Atmospheric Administration, National Weather Service, Office of Meteorology, Fort Worth, Texas.
Schneider, A., Friedl, M.A., Potere, D., 2009. A new map of global urban extent from MODIS satellite data. Environ. Res. Lett. 4 (4), 44003–44011.
Schwartz, J., 2005. Who is sensitive to extremes of temperature?: a case-only analysis. Epidemiology 16 (1), 67–72.
Shindell, D.T., Schmidt, G.A., Miller, R.L., et al., 2001. Northern hemisphere winter climate response to greenhouse gas, ozone, solar, and volcanic forcing. J. Geophys. Res. Amos. 106 (D7), 7193–7210.
Si, P., Zheng, Z., Ren, Y., et al., 2014. Effects of urbanization on daily temperature extremes in North China. J. Geogr. Sci. 24 (2), 349–362.
Statistics Bureau of Guangdong Province, 2014. Guangdong Statistical Yearbook. China Statistics Press, Beijing, China.
Sun, Y., Zhang, X., Zwiers, F.W., et al., 2014. Rapid increase in the risk of extreme summer heat in Eastern China. Nat. Clim. Chang. 4, 1082–1085.
Sun, Y., Zhang, X., Ren, G., et al., 2016. Contribution of urbanization to warming in China. Nat. Clim. Chang. 6, 706–709.
Vautard, R., Cattiaux, J., Yiou, P., et al., 2010. Northern Hemisphere atmospheric stilling partly attributed to an increase in surface roughness. Nat. Geosci. 3 (11), 756–761.
Wang, J., Yan, Z.-W., 2016. Urbanization-related warming in local temperature records: a review. Atmos. Ocean. Sci. Lett. 9 (2), 129–138.
Wang, Z., Ding, Y., He, J., et al., 2004. An updating analysis of the climate change in China in recent 50 years. Acta Meteorol. Sin. 62 (2), 228–236.
Wang, X., Sun, X., Tang, J., et al., 2015. Urbanization-induced regional warming in Yangtze River Delta: potential role of anthropogenic heat release. Int. J. Climatol. 35 (15), 4417–4430.
Xiong, Y., Huang, S., Chen, F., et al., 2012. The impacts of rapid urbanization on the thermal environment: a remote sensing study of Guangzhou, South China. Remote Sens. 4 (7), 2033–2056.
Xu, M., Chang, C.P., Fu, C., et al., 2006. Steady decline of East Asian monsoon winds, 1969–2000: evidence from direct ground measurements of wind speed. J. Geophys. Res. Amos. 111 (D24), D24111.
Xu, Z., Etzel, R.A., Su, H., et al., 2012. Impact of ambient temperature on children's health: a systematic review. Environ. Res. 117, 120–131.
Xu, W., Li, Q., Wang, X.L., et al., 2013. Homogenization of Chinese daily surface air

temperatures and analysis of trends in the extreme temperature indices. J. Geophys. Res. Amos. 118 (17), 9708–9720.
Yang, X., Hou, Y., Chen, B., 2011. Observed surface warming induced by urbanization in East China. J. Geophys. Res. Amos. 116 (D14), D14113.
Yang, X., Leung, R.L., Zhao, N., et al., 2017. Contribution of urbanization to the increase of extreme heat events in an urban agglomeration in East China. Geophys. Res. Lett. 44 (13), 6940–6950.
Ye, J.-S., 2014. Trend and variability of China's summer precipitation during 1955–2008. Int. J. Climatol. 34 (3), 559–566.
Ye, X., Wolff, R., Yu, W., et al., 2012. Ambient temperature and morbidity: a review of epidemiological evidence. Environ. Health Perspect. 120 (1), 19–28.
Ye, J., Li, W., Li, L., et al., 2013. "North drying and south wetting" summer precipitation trend over China and its potential linkage with aerosol loading. Atmos. Res. 125–126, 12–19.
Ye, H., Huang, Z., Huang, L., et al., 2018. Effects of urbanization on increasing heat risks in South China. Int. J. Climatol. https://doi.org/10.1002/joc.5747.
Zanobetti, A., O'Neill, M.S., Gronlund, C.J., et al., 2012. Summer temperature variability and long-term survival among elderly people with chronic disease. Proc. Natl. Acad. Sci. U. S. A. 109 (17), 6608–6613.
Zhai, P., Pan, X., 2003. Trends in temperature extremes during 1951–1999 in China. Geophys. Res. Lett. 30 (17), 1913.
Zhai, P., Zhang, X., Wan, H., et al., 2005. Trends in total precipitation and frequency of daily precipitation extremes over China. J. Clim. 18 (7), 1096–1108.
Zhang, L., Zhang, Z., Wang, C., et al., 2017a. Different mortality effects of extreme temperature stress in three large city clusters of Northern and Southern China. Int. J. Disast. Risk Sci. 8 (4), 445–456.
Zhang, Y., Gao, Z., Pan, Z., et al., 2017b. Spatiotemporal variability of extreme temperature frequency and amplitude in China. Atmos. Res. 185, 131–141.
Zhou, Y., Ren, G., 2011. Change in extreme temperature event frequency over mainland China, 1961–2008. Clim. Res. 50 (2–3), 125–139.
Zhou, L., Dickinson, R.E., Tian, Y., et al., 2004. Evidence for a significant urbanization effect on climate in China. Proc. Natl. Acad. Sci. U. S. A. 101 (26), 9540–9544.
Zhou, L., Dickinson, R.E., Tian, Y., et al., 2007. Impact of vegetation removal and soil aridation on diurnal temperature range in a semiarid region: application to the Sahel. Proc. Natl. Acad. Sci. U. S. A. 104 (46), 17937–17942.
Zhou, B., Xu, Y., Wu, J., et al., 2016. Changes in temperature and precipitation extreme indices over China: analysis of a high-resolution grid dataset. Int. J. Climatol. 36 (3), 1051–1066.